Quantum Criticality in Open Quantum Spin Chains with Nonreciprocity

Samuel E. Begg [1,*] and Ryo Hanai [1,2,†]
[1] *Asia Pacific Center for Theoretical Physics, Pohang 37673, Korea*
[2] *Center for Gravitational Physics and Quantum Information, Yukawa Institute for Theoretical Physics, Kyoto University, Kyoto 606-8502, Japan*

(Received 21 July 2023; revised 26 December 2023; accepted 20 February 2024; published 20 March 2024)

We investigate the impact of nonreciprocity on universality and critical phenomena in open quantum interacting many-body systems. Nonreciprocal open quantum systems often have an exotic spectral sensitivity to boundary conditions, known as the Liouvillian skin effect (LSE). By considering an open quantum XXZ spin chain that exhibits LSE, we demonstrate the existence of a universal scaling regime that is *not* affected by the presence of the LSE. We resolve the critical exponents, which differ from those of free fermions, via tensor network methods and demonstrate that observables exhibit a universal scaling collapse, irrespective of the reciprocity. We find that the LSE only becomes relevant when a healing length scale ξ_{heal} at the system's edge (which is different from the localization length of the eigenstate of the Liouvillian) exceeds the system size, allowing edge properties to dominate the physics. We expect this result to be a generic feature of nonreciprocal models in the vicinity of a critical point. The driven-dissipative quantum criticality we observe has no classical analog and stems from the existence of multiple dark states.

DOI: 10.1103/PhysRevLett.132.120401

Introduction.—Universality in nonequilibrium systems can be seen in numerous phenomena ranging from directed percolation [1], flocking [2–4], Kardar-Parisi-Zhang physics [5] observed in various platforms [6–16], and nonreciprocal phase transitions [17–23]. Recent advances in open quantum systems offer an exciting avenue for extending this concept. This is exemplified by criticality in non-Hermitian systems [24,25], open quantum systems [19,20,26–46], and measurement-induced phase transitions [47,48]. Engineered nonreciprocal couplings provide a promising direction for furthering these investigations. A number of platforms [49–55], including an optomechanical circuit [49] and cold atoms [50,54], have demonstrated that asymmetric (nonreciprocal) transport can be engineered [56–68]. Surprisingly, the spectrum of a system of particles hopping asymmetrically on a lattice exhibits extreme sensitivity to changes in the boundary conditions, known as the non-Hermitian skin effect [69–82] or Liouvillian skin effect (LSE) in the context of open quantum systems [57,63,66–68]. As spectral properties are usually a key element in determining the behavior of observables, one might expect that the presence of the LSE drastically alters the physics and hence the universal features (as was indeed shown in several works [63,68,83]).

In this Letter, we introduce a nonreciprocal open quantum spin system that exhibits universal properties that are *unaffected* by the LSE. For equilibrium critical phenomena, generic observables follow a universal power law as a function of the distance to the critical point $|T - T_c|$ (e.g., $C_{\mathrm{V}} \sim |T - T_c|^{-\alpha}$, where C_{V} is the specific heat and α is a critical exponent). This Letter considers an analogous situation in a nonreciprocal open quantum spin system exhibiting a quantum critical point. As the parameter Γ controlling the distance to the critical point is reduced, we observe universal behavior (e.g., $M \sim \Gamma^{\alpha} + \mathrm{const}$, where M is the magnetization) that is *independent* of the strength of the nonreciprocity, contrary to the expectation given by a strong spectral sensitivity to boundary conditions. Quantum criticality is demonstrated by the scaling collapse of observables, which exhibit the same critical exponents across various microscopic parameters. The resolved critical exponents differ from free systems, which we attribute to many-body interaction effects. We find that the LSE only impacts the bulk physics in the regime where the healing length ξ_{heal} at the edge of the system (that diverges at the critical point $\Gamma \to 0$) exceeds the size of the system. This length scale ξ_{heal} is different from the localization scale of the eigenmodes of the Liouvillian [65]. We expect LSE-independent universality to be generic for nonreciprocal systems near a critical point.

Critical dynamics with nonreciprocity.—To study the effect of nonreciprocity on universality, we consider a quantum spin system whose interactions are reservoir-engineered to be nonreciprocal. The evolution of the system's density matrix $\hat{\rho}$ in the presence of Markovian dissipation obeys the Lindblad master equation [84]

$$\frac{d\hat{\rho}(t)}{dt} = \mathcal{L}[\hat{\rho}] = -i[\hat{H}, \hat{\rho}(t)] + \sum_j \hat{\mathcal{D}}_j[\hat{\rho}(t)], \qquad (1)$$

with dissipators $\hat{\mathcal{D}}_j[\cdot] = \hat{L}_j[\cdot]\hat{L}_j^{\dagger} - \frac{1}{2}\{\hat{L}_j^{\dagger}\hat{L}_j, [\cdot]\}$ at site j. We solve Eq. (1) using time-evolving block decimation

© 2024 American Physical Society

(TEBD) [85–87]; see Supplemental Material (SM) [88] for details and Refs. [96–107] for examples of tensor networks applied to open quantum systems. We focus on the paradigmatic quantum XXZ spin Hamiltonian

$$\hat{H} = J\sum_j \left(\frac{1}{2}(\hat{S}_j^- \hat{S}_{j+1}^+ + \hat{S}_j^+ \hat{S}_{j+1}^-) + \Delta \hat{S}_j^z \hat{S}_{j+1}^z\right), \quad (2)$$

where J and Δ are the exchange interaction and anisotropy, respectively. The spin-1/2 operators obey $[\hat{S}_i^a, \hat{S}_j^b] = i\delta_{ij}\epsilon_j^{abc}\hat{S}_j^c$, and we set $\hbar = 1$. To study the nonreciprocal interaction effects, we use the dissipator

$$\hat{L}_j^l = \sqrt{\kappa}(\hat{S}_j^- + e^{i\phi}\hat{S}_{j+1}^-). \quad (3)$$

In the SM [88], we provide a concrete proposal for implementing this correlated dissipation in a trapped ions platform using dissipative Aharanov-Bohm rings [56,108], utilizing recent experimental advances [109–111]. It becomes clear that the dissipator (3) gives rise to a nonreciprocal interaction [Fig. 1(a)] by considering the conditional Hamiltonian, $\hat{H}_{\rm cd} = \hat{H} - (i/2)\sum_j \hat{L}_j^{l\dagger}\hat{L}_j^l$, governing the evolution in the absence of quantum jumps:

$$\hat{H}_{\rm cd} = \sum_j \frac{J_+}{2}\hat{S}_j^- \hat{S}_{j+1}^+ + \frac{J_-}{2}\hat{S}_j^+ \hat{S}_{j+1}^- + J\Delta \hat{S}_j^z \hat{S}_{j+1}^z - i\kappa \hat{S}_j^+ \hat{S}_j^-,$$

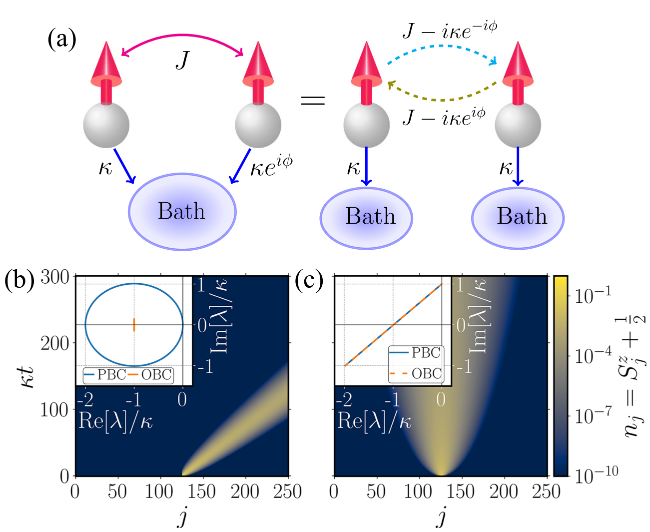

FIG. 1. (a) Left: two quantum spins coupled to a bath with coupling strength κ. The bath acts on the spins as $\hat{L}_j^l = \sqrt{\kappa}(\hat{S}_j^- + e^{i\phi}\hat{S}_{j+1}^-)$. Right: the phase $e^{i\phi}$ causes interference that results in an effective system of nonreciprocally interacting spins and additional local on-site baths. (b) Relaxation of magnetization from the initial state with a single up spin in the center of the chain for a nonreciprocal ($\phi = -\pi/2$) XX spin chain ($\Delta = 0$) with open boundary conditions. (c) The same for the reciprocal case ($\phi = 0$). Insets: the spectrum λ of the Liouvillian $\mathcal{L}$ in the single-magnon sector for periodic and open boundary conditions. We set $J/\kappa = 1$ [113].

where $J_\pm = J - ie^{\mp i\phi}\kappa$. The phase factor $e^{i\phi}$ in Eq. (3) therefore controls the nonreciprocity of interactions between nearest neighbor sites. The conditional Hamiltonian is similar to the non-Hermitian XXZ model considered in Ref. [112]. We stress, however, that we will investigate the unconditional dynamics including the effects of quantum jumps.

Figure 1(b) [Fig. 1(c)] demonstrates the anticipated nonreciprocal (reciprocal) transport of a spin excitation for $\phi = -\pi/2$ ($\phi = 0$). Here, the spatial magnetization profile $S_j^z = \langle \hat{S}_j^z \rangle$ is plotted (with an offset for the ease of visibility), computed with open boundary conditions (OBC). A spectral sensitivity to boundary conditions (i.e., LSE [57,63]) in the nonreciprocal case is also observed [see insets of Figs. 1(b) and 1(c)], as expected.

Interestingly, the relaxation of the system is far slower than the scales set by $\mathcal{O}(J^{-1})$ and $\mathcal{O}(\kappa^{-1})$ and is, in fact, algebraic (see Fig. 4), indicating that the system is critical. The slow relaxation occurs due to the presence of a dark state other than the all down state $|\Downarrow\rangle = \prod_j |\downarrow\rangle_j$. To see this, let us temporarily assume a periodic boundary condition (PBC) and Fourier transform the dissipation terms in the Lindblad equation (1), giving

$$\sum_j \hat{\mathcal{D}}_j[\hat{\rho}] = \sum_k \kappa(k)\left(\hat{S}_k^- \hat{\rho}\hat{S}_k^+ - \frac{1}{2}\{\hat{S}_k^+ \hat{S}_k^-, \hat{\rho}\}\right), \quad (4)$$

where $\kappa(k) = 2\kappa(1 + \cos(k + \phi))$. Since the dissipator Eq. (3) involves only spin flips from up to down, the system trivially possesses a dark state with all spins down $|\Downarrow\rangle$, i.e., $\mathcal{L}[|\Downarrow\rangle\langle\Downarrow|] = 0$. Notice, however, that the dissipation vanishes at $k = k^* = \pi - \phi$. This implies that a state $|D_k\rangle \equiv \hat{S}_k^+|\Downarrow\rangle$ does not experience *any* dissipation at $k = k_*$, where the operator $\hat{S}_k^+ = (1/\sqrt{L})\sum_{j=1}^L e^{ikj}\hat{S}_j^+$ creates a spin-wave mode with momentum k. It can readily be shown that this is simultaneously an eigenstate of the Hamiltonian Eq. (2), which is a consequence of U(1) symmetry, making it a dark state $\mathcal{L}[|D_{k_*}\rangle\langle D_{k_*}|] = 0$ [88]. For k very close to but not *exactly* at $k = k_*$, $|D_k\rangle$ experiences a vanishingly small (but finite) dissipation rate [114]. This implies that the characteristic timescale of the dissipation is divergent in the thermodynamic limit, meaning that the dynamics are critical, in agreement with Figs. 1(b) and 1(c).

The numerical results in Figs. 1(b) and 1(c) are obtained with OBC, while Eq. (4) is obtained under PBC. The two results are consistent with each other, despite the presence (absence) of the gap in the Liouvillian spectrum for OBC (PBC) [see Figs. 1(b) and 1(c) insets], because the local spin excitation will not know about the boundary conditions until they propagate or diffuse to hit the boundary [65,67]. This provides a key intuition: the *spectral* sensitivity to boundary conditions does not necessarily imply the sensitivity for *observables*.

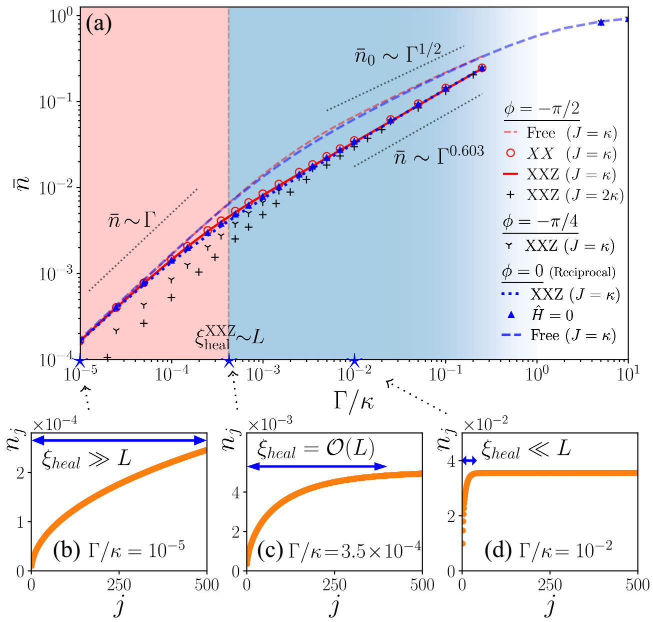

FIG. 2. (a) Excitation density $\bar{n}$ vs Γ in the steady state for different parameters. Results are displayed for the following nonreciprocal ($\phi = -\pi/2$) systems: XXZ ($\Delta = 2$), XX ($\Delta = 0$), and free fermions for $L = 500$, as well as XXZ with $J/\kappa = 2$ ($\Delta = 1$) for $L = 100$. For $\phi = -\pi/4$ we show XXZ ($\Delta = 2$) with $L = 100$. Reciprocal ($\phi = 0$) XXZ ($\Delta = 2$), $\hat{H} = 0$, and free fermion results are also shown, all with $L = 50$. Various fits $\bar{n} \sim \Gamma^{\alpha}$ are displayed (discussion in the text). (b)–(d) Steady-state excitation density n_j for different Γ/κ, corresponding to the red region $\xi_{\rm heal} \ll L$ (a), the transition regime $\xi_{\rm heal} \sim L$ (b), and the asymptotic region $\xi_{\rm heal} \gg L$ (c), respectively. The data corresponds to the nonreciprocal case with $\Delta = 0$ and $L = 500$.

In addition to the above-introduced engineered loss [Eq. (3)], we further add a uniform gain to the system, $\hat{L}_j^g = \sqrt{\Gamma}\hat{S}_j^+$ [115]. This term invalidates the discussion above, introducing an additional timescale $\mathcal{O}(\Gamma^{-1})$ to the system. Therefore, Γ acts as a parameter that controls the distance from the critical point. Remarkably, despite the spectral sensitivity in the nonreciprocal case, which persists even for finite Γ (see SM [88]), we will show that nonreciprocal and reciprocal systems display *identical* universal properties in asymptotic regimes.

It is instructive to compare this model to a similar nonreciprocal free fermion model studied in Refs. [57,64,65]

$$\hat{H}_0 = \sum_j \frac{J}{2}(\hat{c}_j^\dagger \hat{c}_{j+1} + \hat{c}_{j+1}^\dagger \hat{c}_j), \qquad \hat{L}_j^{l0} = \sqrt{\kappa}(\hat{c}_j + e^{i\phi}\hat{c}_{j+1}), \tag{5}$$

and $\hat{L}_j^{g0} = \sqrt{\Gamma}\hat{c}_j^\dagger$, where $\hat{c}_j$ is a fermionic annihilation operator satisfying $\{\hat{c}_i, \hat{c}_j^\dagger\} = \delta_{ij}$, and $\{\hat{c}_i^\dagger, \hat{c}_j^\dagger\} = \{c_i, c_j\} = 0$. The conditional Hamiltonian $\hat{H}_{\rm cd}^0 = \hat{H}_0 - (i/2)\sum_j \hat{L}_j^{l0\dagger}\hat{L}_j^{l0}$ for this model ($\Gamma = 0$ for simplicity) is given by the so-called Hatano-Nelson model [116,117],

$$\hat{H}_{\rm cd}^0 = \sum_j \frac{J_+}{2}\hat{c}_{j+1}^\dagger \hat{c}_j + \frac{J_-}{2}\hat{c}_j^\dagger \hat{c}_{j+1} - i\kappa \hat{n}_j, \tag{6}$$

where $\hat{n}_j = \hat{c}_j^\dagger \hat{c}_j$ is the density operator. Equation (6) describes asymmetric hopping with an additional imaginary term. A more direct comparison to our spin model can be made by performing the Jordan-Wigner transformation [118] for OBC, defined as $\hat{S}_j^+ = e^{-i\pi \sum_i^{j-1} \hat{c}_i^\dagger \hat{c}_i}\hat{c}_j^\dagger$, $\hat{S}_j^- = e^{i\pi \sum_i^{j-1} \hat{c}_i^\dagger \hat{c}_i}\hat{c}_j$, $\hat{S}_j^z = \hat{n}_j - \frac{1}{2}$. The jump operator (3) and conditional Hamiltonian then take the form

$$\hat{L}_j^l = \sqrt{\kappa}\left(e^{i\pi \sum_i^{j-1} \hat{c}_i^\dagger \hat{c}_i}\hat{c}_j + e^{i\phi} e^{i\pi \sum_i^{j} \hat{c}_i^\dagger \hat{c}_i}\hat{c}_{j+1}\right), \tag{7}$$

$$\hat{H}_{\rm cd} = \hat{H}_{\rm cd}^0 + J\Delta\left(\hat{n}_j \hat{n}_{j+1} - \hat{n}_j + \frac{1}{4}\right), \tag{8}$$

where one sees that $\hat{H}_{\rm cd}$ is given by the Hatano-Nelson model (6) extended to have nearest-neighbor interactions, suggesting that the free fermion model [Eq. (5)] can be regarded as the noninteracting limit of our spin model and serves as a useful point of reference. Note that, while the string operators $e^{\pm i\pi \sum_i^{j-1} \hat{c}_i^\dagger \hat{c}_i}$ in the conditional Hamiltonian (8) have cancelled out, those in the quantum jump term $\hat{L}_j^l \hat{\rho}(t) \hat{L}_j^{l\dagger}$ cannot be removed. This means that even the XX model case $\Delta = 0$ does *not* correspond to a free system.

Universality and scaling collapse.—Figure 2(a) shows the spatially averaged excitation number $\bar{n} = (1/L)\sum_j n_j$ in the steady state as a function of Γ, where $n_j = \langle \hat{n}_j \rangle = \langle \hat{S}_j^z \rangle + \frac{1}{2}$. Here, data is shown for a variety of parameters, including different strength of nonreciprocity ϕ, Δ, J. Data for different system sizes is in the SM [88]. For comparison, the free fermion case is also plotted. Consistent with the property that $\Gamma = 0$ is a critical point, we observe the power-law scaling $\bar{n} \sim \Gamma^{\alpha}$. Remarkably, the exponent $\alpha = 0.603(9)$ in the blue shaded region is identical in all cases, including both nonreciprocal ($\phi = -\pi/2$) and reciprocal ($\phi = 0$) cases for XXZ ($\Delta > 0$) and XX models ($\Delta = 0$), different exchange interaction strengths J, and even a purely dissipative case ($\hat{H} = 0$). The obtained exponent $\alpha = 0.603(9)$ is different from the free fermion case $\alpha = 0.5$. The result clearly demonstrates that universal features have emerged, irrespective of the presence of the LSE. For the purely dissipative case ($\hat{H} = 0$), ϕ can be removed from the Liouvillian (1) via a local gauge transformation $\hat{S}_j^- \to e^{-i\phi j}\hat{S}_j^-$, further illustrating that the scaling is independent of reciprocity.

Figure 3 demonstrates a scaling collapse of the density and the spatial correlation function in this region:

$$n_j(t, \Gamma) = t^{-\alpha/\nu z} f_{n_j}(t\Gamma^{\nu z}), \tag{9}$$

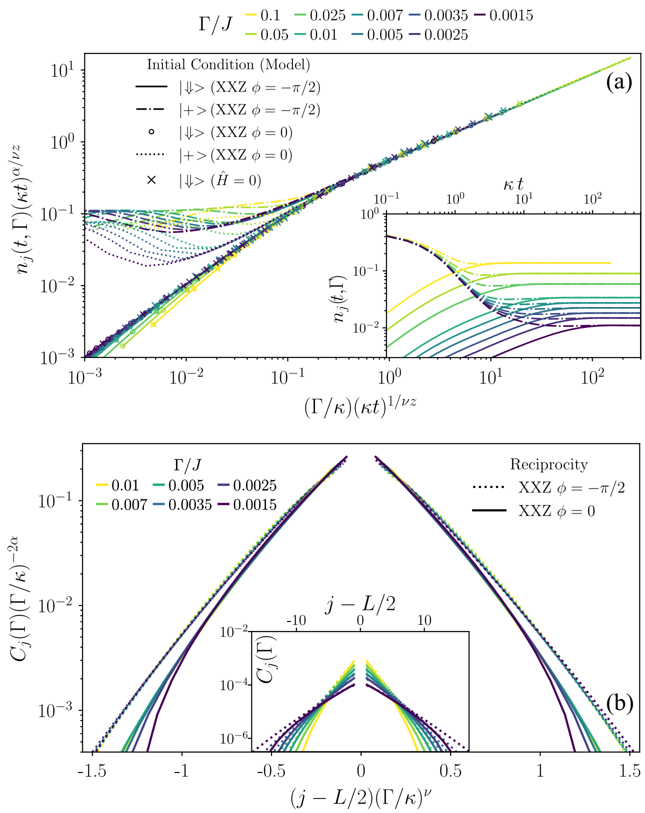

FIG. 3. (a) $n_j(t,\Gamma)(\kappa t)^{\alpha/\nu z}$ vs $(\Gamma/\kappa)(\kappa t)^{1/\nu z}$ with $\alpha = 0.603$, $\nu = 0.386$, and $z = 1.96$ for the $J/\kappa = 1$, $\Delta = 2$, dissipative XXZ model over a range of Γ values, with $L = 500$ and setting $j = 475$. Results are displayed for nonreciprocal ($\phi = -\pi/2$), reciprocal ($\phi = 0$), and $\hat{H} = 0$ cases, with initial conditions being the fully polarized state $|\Downarrow\rangle$ and the x-polarized state $\prod_j^L |+\rangle_j$, respectively. The inset shows unscaled data for the nonreciprocal cases. (b) Scaled connected correlation $C_j(\Gamma)(\Gamma/\kappa)^{-2\alpha}$ vs $(j - L/2)(\Gamma/\kappa)^{\nu}$ in the steady state for a range of Γ values. The inset shows the unscaled data.

$$C_j(\Gamma) = \Gamma^{2\alpha} f_{C_j}\left[\Gamma^{\nu}(j - L/2)\right], \tag{10}$$

where $C_j(\Gamma)$ is the magnitude of connected correlations between a site j and the center of the chain $L/2$, $C_j(\Gamma) = |\langle \hat{S}^z_{L/2}\hat{S}^z_j\rangle - \langle \hat{S}^z_{L/2}\rangle\langle \hat{S}^z_j\rangle|$. Here, $f_{n_j}(x)$, $f_{C_j}(x)$ are scaling functions for the density and spatial correlation function, respectively, while α, z and ν are critical exponents that characterize the universal features. Data is provided for reciprocal and nonreciprocal cases and for different parameters and initial states. The scaling collapse is achieved, by setting the critical exponents $\{z, \nu, \alpha\} = \{1.96(13), 0.386(16), 0.603(9)\}$ [119], unambiguously demonstrating the emergence of universality. For the free fermions we find $\{z, \nu, \alpha\} = \{2, 0.5, 0.5\}$ [88]. The critical phenomenon we observe is similar to the quantum critical phenomena proposed in Refs. [40,41] for a driven-dissipative bosonic system. However, their system has a steady state that is interacting, while our steady state at the critical point is a vacuum, resulting in a different universality class characterized by critical exponents $\{z, \nu, \alpha\} = \{2.025, 0.405, 0.5\}$.

In the regime of sufficiently small $\Gamma \lesssim J/L$ [the region shaded in red in Fig. 2(a)], we observe that the scaling properties change to $\bar{n} \sim \Gamma^{\alpha'} = \Gamma$, i.e., $\alpha' = 1$. (Note however that this regime shrinks to measure zero as the system size is increased.) This can be understood from the steady-state density profile n_j in Figs. 2(b)–2(d), which shows results for different Γ values. As seen, the density profile exhibits a dip at the left boundary, with its healing length ξ_{heal} (characterizing the length of the dip) decreasing as a function of Γ. The dip arises because sites near the left boundary do not experience any flux of incoming excitations from the boundary, whereas sites in the bulk are "topped up" from their left. As these spin waves exhibit an increasingly long lifetime as Γ decreases, the healing length ξ_{heal} becomes increasingly long and diverges at $\Gamma \to 0$. Note that $\xi_{\mathrm{heal}} \propto \Gamma^{-1}$ is very different from the localization length ξ_{loc} of the eigenmodes of the Liouvillian $\mathcal{L}$, which is solely determined by the asymmetry of the hopping $\xi_{\mathrm{loc}} \sim 1/\log(|J_+|/|J_-|)$ [65].

In the asymptotic regime ($J/L \lesssim \Gamma \lesssim \kappa$) [Fig. 2(d)], the healing length ξ_{heal} is small compared to the system size L. Therefore, the density profile is almost uniform. As Γ decreases to $\Gamma \lesssim J/L$ the healing length starts to exceed the system size [Figs. 2(b) and 2(c)]. This implies that, while in the asymptotic region $J/L \lesssim \Gamma \lesssim \kappa$, the physics is determined by the *bulk* properties (that do not care about LSE [65,122]), the region with $\Gamma \lesssim J/L$ is dominated by the *edge* properties, giving a natural explanation for the change of scaling properties at different regimes. The scaling $\bar{n} \sim \Gamma$ is consistent with the free fermion case with perfect nonreciprocity ($\phi = -\pi/2$, $J = \kappa$) for $\xi_{\mathrm{heal}} \gg L$ [65]. Interestingly, while in this limit the transition between the two regimes occurs at $\Gamma = \mathcal{O}(v_g/L)$ for free fermions, for the spin systems, the many-body interaction alters the scaling to $\Gamma = \mathcal{O}(v_g/L^{1.25})$, where $v_g = J\sin(\pi - \phi)$ is the group velocity of the least damped mode k_*.

The scaling properties in the region $\Gamma \lesssim J/L$ are strongly affected by the LSE. This is demonstrated in Fig. 4(a), which shows a space-time plot of the excitation density for $\Gamma = 0$, starting from an initially fully polarized state with all spins up $|\Uparrow\rangle$. Here, the excitation density $n_j(t)$ exhibits a sudden transition from power law to exponential decay [57,63,66]. This occurs when site j is no longer "topped up" by incoming excitations: all the long-lived excitations that were initially left of site j have propagated to its right [67]. For sites near the right edge, which are last to relax, this takes a time t_r proportional to the system size, i.e., $t_r \sim \xi^{z'} = L$ ($z' = 1$). In comparison, the transport is approximately diffusive in the reciprocal case ($z' \approx 2$), which is clearly visible in Fig. 1(c). Therefore, in the region $\Gamma \lesssim J/L$ the scaling is altered by the LSE. In the

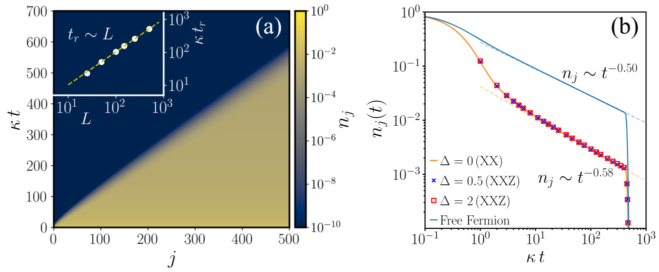

FIG. 4. (a) Space-time plot of the particle density n_j for the nonreciprocal ($\phi = -\pi/2$) XXZ spin chain with $L = 500$ sites, starting from all spins up and with $\Gamma = 0$, $J/\kappa = 1$, $\Delta = 2$. Inset: the relaxation time to the steady state, t_r, vs system size L, with linear fit $t_r \sim L$ (dotted). (b) Density decay n_j vs time with $j = 450$, for various system parameters.

SM [88], we show for the free fermion system that under PBC this region only arises for $\Gamma \leq \mathcal{O}(1/L^2)$.

Finally, Fig. 4(b) shows that many-body effects also alter the power-law exponent $\chi = 0.58$ of $n_j(t) \sim t^{-\chi}$ at $\Gamma = 0$ from the free fermion result $\chi = 0.5$. Curiously, χ is found to be initial-state-dependent ranging from $\chi = 0.5$ to 0.58 [88]. Clarifying the origin of this remains our future work.

Discussion.—In conclusion, we have demonstrated the existence of a Liouvillian skin effect (LSE) independent universal regime. We showed that the LSE can affect the bulk properties only when $\xi_{\text{heal}} \gtrsim \mathcal{O}(L)$. The LSE-induced transition of scaling reported in Refs. [63,83] corresponds to the latter regime where the number conservation in their model implies the absence of characteristic length scales (similar to "model B" of Ref. [123]).

We thank Aashish Clerk, Kazuya Fujimoto, Tomohiro Sasamoto, and Hironobu Yoshida for useful discussions and Hosho Katsura and Alexander McDonald for the critical reading of the manuscript. This work was supported by an appointment to the JRG program at the APCTP through the Science and Technology Promotion Fund and Lottery Fund of the Korean Government, as well as by Grant-in-Aid for Research Activity Start-up from JSPS in Japan (Grant No. 23K19034), and by the National Research Foundation (NRF) funded by the Ministry of Science of Korea (Grant No. RS-2023-00249900). S. E. B. acknowledges the support of the Young Scientist Training Program at the Asia Pacific Center for Theoretical Physics.

*samuel.begg@apctp.org
†ryo.hanai@yukawa.kyoto-u.ac.jp, ryo.hanai@apctp.org

[1] H. Hinrichsen, Adv. Phys. **49**, 815 (2000).
[2] T. Vicsek, A. Czirók, E. Ben-Jacob, I. Cohen, and O. Shochet, Phys. Rev. Lett. **75**, 1226 (1995).
[3] J. Toner and Y. Tu, Phys. Rev. Lett. **75**, 4326 (1995).
[4] B. Mahault, F. Ginelli, and H. Chaté, Phys. Rev. Lett. **123**, 218001 (2019).
[5] M. Kardar, G. Parisi, and Y.-C. Zhang, Phys. Rev. Lett. **56**, 889 (1986).
[6] F. Spitzer, Adv. Math. **5**, 246 (1970).
[7] T. Kriecherbauer and J. Krug, J. Phys. A **43**, 403001 (2010).
[8] K. A. Takeuchi and M. Sano, Phys. Rev. Lett. **104**, 230601 (2010).
[9] K. A. Takeuchi, Physica (Amsterdam) **504A**, 77 (2018).
[10] M. Ljubotina, M. Žnidarič, and T. Prosen, Nat. Commun. **8**, 16117 (2017).
[11] M. Ljubotina, M. Žnidarič, and T. Prosen, Phys. Rev. Lett. **122**, 210602 (2019).
[12] A. Scheie, N. E. Sherman, M. Dupont, S. Nagler, M. B. Stone, G. E. Granroth, J. E. Moore, and D. A. Tennant, Nat. Phys. **17**, 726 (2021).
[13] E. Ilievski, J. De Nardis, S. Gopalakrishnan, R. Vasseur, and B. Ware, Phys. Rev. X **11**, 031023 (2021).
[14] B. Ye, F. Machado, J. Kemp, R. B. Hutson, and N. Y. Yao, Phys. Rev. Lett. **129**, 230602 (2022).
[15] D. Wei, A. Rubio-Abadal, B. Ye, F. Machado, J. Kemp, K. Srakaew, S. Hollerith, J. Rui, S. Gopalakrishnan, N. Y. Yao, I. Bloch, and J. Zeiher, Science **376**, 716 (2022).
[16] Q. Fontaine, D. Squizzato, F. Baboux, I. Amelio, A. Lemaître, M. Morassi, I. Sagnes, L. Le Gratiet, A. Harouri, M. Wouters, I. Carusotto, A. Amo, M. Richard, A. Minguzzi, L. Canet, S. Ravets, and J. Bloch, Nature (London) **608**, 687 (2022).
[17] M. Fruchart, R. Hanai, P. B. Littlewood, and V. Vitelli, Nature (London) **592**, 363 (2021).
[18] R. Hanai, A. Edelman, Y. Ohashi, and P. B. Littlewood, Phys. Rev. Lett. **122**, 185301 (2019).
[19] R. Hanai and P. B. Littlewood, Phys. Rev. Res. **2**, 033018 (2020).
[20] C. P. Zelle, R. Daviet, A. Rosch, and S. Diehl, arXiv: 2304.09207.
[21] Ezequie I. Rodriguez Chiacchio, A. Nunnenkamp, and M. Brunelli, Phys. Rev. Lett. **131**, 113602 (2023).
[22] Z. You, A. Baskaran, and M. C. Marchetti, Proc. Natl. Acad. Sci. U.S.A. **117**, 19767 (2020).
[23] S. Saha, J. Agudo-Canalejo, and R. Golestanian, Phys. Rev. X **10**, 041009 (2020).
[24] Y. Ashida, S. Furukawa, and M. Ueda, Nat. Commun. **8**, 15791 (2017).
[25] M. Nakagawa, N. Kawakami, and M. Ueda, Phys. Rev. Lett. **121**, 203001 (2018).
[26] A. Mitra, S. Takei, Y. B. Kim, and A. J. Millis, Phys. Rev. Lett. **97**, 236808 (2006).
[27] T. Prosen and I. Pižorn, Phys. Rev. Lett. **101**, 105701 (2008).
[28] S. Diehl, A. Tomadin, A. Micheli, R. Fazio, and P. Zoller, Phys. Rev. Lett. **105**, 015702 (2010).
[29] E. G. Dalla Torre, E. Demler, T. Giamarchi, and E. Altman, Nat. Phys. **6**, 806 (2010).
[30] D. Nagy, G. Szirmai, and P. Domokos, Phys. Rev. A **84**, 043637 (2011).
[31] B. Öztop, M. Bordyuh, Ö. E. Müstecaplıoğlu, and H. E. Türeci, New J. Phys. **14**, 085011 (2012).

[32] Emanuele G. Dalla Torre, S. Diehl, M. D. Lukin, S. Sachdev, and P. Strack, Phys. Rev. A **87**, 023831 (2013).
[33] L. M. Sieberer, S. D. Huber, E. Altman, and S. Diehl, Phys. Rev. Lett. **110**, 195301 (2013).
[34] Z. Cai and T. Barthel, Phys. Rev. Lett. **111**, 150403 (2013).
[35] M. Marcuzzi, E. Levi, S. Diehl, J. P. Garrahan, and I. Lesanovsky, Phys. Rev. Lett. **113**, 210401 (2014).
[36] U. C. Täuber and S. Diehl, Phys. Rev. X **4**, 021010 (2014).
[37] L. He, L. M. Sieberer, E. Altman, and S. Diehl, Phys. Rev. B **92**, 155307 (2015).
[38] M. Buchhold and S. Diehl, Phys. Rev. A **92**, 013603 (2015).
[39] M. F. Maghrebi and A. V. Gorshkov, Phys. Rev. B **93**, 014307 (2016).
[40] J. Marino and S. Diehl, Phys. Rev. Lett. **116**, 070407 (2016).
[41] J. Marino and S. Diehl, Phys. Rev. B **94**, 085150 (2016).
[42] L. M. Sieberer, M. Buchhold, and S. Diehl, Rep. Prog. Phys. **79**, 096001 (2016).
[43] M. Foss-Feig, P. Niroula, J. T. Young, M. Hafezi, A. V. Gorshkov, R. M. Wilson, and M. F. Maghrebi, Phys. Rev. A **95**, 043826 (2017).
[44] D. Nigro, D. Rossini, and E. Vicari, Phys. Rev. A **100**, 052108 (2019).
[45] J. T. Young, A. V. Gorshkov, M. Foss-Feig, and M. F. Maghrebi, Phys. Rev. X **10**, 011039 (2020).
[46] K. Fujimoto, R. Hamazaki, and Y. Kawaguchi, Phys. Rev. Lett. **129**, 110403 (2022).
[47] B. Skinner, J. Ruhman, and A. Nahum, Phys. Rev. X **9**, 031009 (2019).
[48] M. P. A. Fisher, V. Khemani, A. Nahum, and S. Vijay, Annu. Rev. Condens. Matter Phys. **14**, 335 (2023).
[49] K. Fang, J. Luo, A. Metelmann, M. H. Matheny, F. Marquardt, A. A. Clerk, and O. Painter, Nat. Phys. **13**, 465 (2017).
[50] W. Gou, T. Chen, D. Xie, T. Xiao, T.-S. Deng, B. Gadway, W. Yi, and B. Yan, Phys. Rev. Lett. **124**, 070402 (2020).
[51] L. Xiao, T. Deng, K. Wang, G. Zhu, Z. Wang, W. Yi, and P. Xue, Nat. Phys. **16**, 761 (2020).
[52] L. Xiao, T. Deng, K. Wang, Z. Wang, W. Yi, and P. Xue, Phys. Rev. Lett. **126**, 230402 (2021).
[53] Q. Lin, T. Li, L. Xiao, K. Wang, W. Yi, and P. Xue, Nat. Commun. **13**, 3229 (2022).
[54] Q. Liang, D. Xie, Z. Dong, H. Li, H. Li, B. Gadway, W. Yi, and B. Yan, Phys. Rev. Lett. **129**, 070401 (2022).
[55] Q. Lin, W. Yi, and P. Xue, Nat. Commun. **14**, 6283 (2023).
[56] A. Metelmann and A. A. Clerk, Phys. Rev. X **5**, 021025 (2015).
[57] F. Song, S. Yao, and Z. Wang, Phys. Rev. Lett. **123**, 170401 (2019).
[58] F. Minganti, A. Miranowicz, R. W. Chhajlany, and F. Nori, Phys. Rev. A **100**, 062131 (2019).
[59] C.-H. Liu, K. Zhang, Z. Yang, and S. Chen, Phys. Rev. Res. **2**, 043167 (2020).
[60] S. Longhi, Phys. Rev. B **102**, 201103(R) (2020).
[61] C. C. Wanjura, M. Brunelli, and A. Nunnenkamp, Nat. Commun. **11**, 3149 (2020).
[62] N. Okuma and M. Sato, Phys. Rev. B **103**, 085428 (2021).
[63] T. Haga, M. Nakagawa, R. Hamazaki, and M. Ueda, Phys. Rev. Lett. **127**, 070402 (2021).
[64] C. C. Wanjura, M. Brunelli, and A. Nunnenkamp, Phys. Rev. Lett. **127**, 213601 (2021).
[65] A. McDonald, R. Hanai, and A. A. Clerk, Phys. Rev. B **105**, 064302 (2022).
[66] F. Yang, Q.-D. Jiang, and E. J. Bergholtz, Phys. Rev. Res. **4**, 023160 (2022).
[67] G. Lee, A. McDonald, and A. Clerk, Phys. Rev. B **108**, 064311 (2023).
[68] Y.-M. Hu, W.-T. Xue, F. Song, and Z. Wang, Phys. Rev. B **108**, 235422 (2023).
[69] T. E. Lee, Phys. Rev. Lett. **116**, 133903 (2016).
[70] S. Yao and Z. Wang, Phys. Rev. Lett. **121**, 086803 (2018).
[71] F. K. Kunst, E. Edvardsson, J. C. Budich, and E. J. Bergholtz, Phys. Rev. Lett. **121**, 026808 (2018).
[72] Y. Xiong, J. Phys. Commun. **2**, 035043 (2018).
[73] A. McDonald, T. Pereg-Barnea, and A. A. Clerk, Phys. Rev. X **8**, 041031 (2018).
[74] L. Herviou, J. H. Bardarson, and N. Regnault, Phys. Rev. A **99**, 052118 (2019).
[75] D. S. Borgnia, A. J. Kruchkov, and R.-J. Slager, Phys. Rev. Lett. **124**, 056802 (2020).
[76] N. Okuma, K. Kawabata, K. Shiozaki, and M. Sato, Phys. Rev. Lett. **124**, 086801 (2020).
[77] X. Zhang, T. Zhang, M.-H. Lu, and Y.-F. Chen, Adv. Phys. **7**, 2109431 (2022).
[78] Z. Gong, Y. Ashida, K. Kawabata, K. Takasan, S. Higashikawa, and M. Ueda, Phys. Rev. X **8**, 031079 (2018).
[79] K. Kawabata, S. Higashikawa, Z. Gong, Y. Ashida, and M. Ueda, Nat. Commun. **10**, 297 (2019).
[80] H. Zhou and J. Y. Lee, Phys. Rev. B **99**, 235112 (2019).
[81] K. Kawabata, K. Shiozaki, M. Ueda, and M. Sato, Phys. Rev. X **9**, 041015 (2019).
[82] Y. Ashida, Z. Gong, and M. Ueda, Adv. Phys. **69**, 249 (2020).
[83] K. Kawabata, T. Numasawa, and S. Ryu, Phys. Rev. X **13**, 021007 (2023).
[84] G. Lindblad, Commun. Math. Phys. **48**, 119 (1976).
[85] G. Vidal, Phys. Rev. Lett. **93**, 040502 (2004).
[86] U. Schollwöck, Ann. Phys. (N.Y.) **326**, 96 (2011).
[87] S. Paeckel, T. Köhler, A. Swoboda, S. R. Manmana, U. Schollwöck, and C. Hubig, Ann. Phys. (N.Y.) **411**, 167998 (2019).
[88] See Supplemental Material at http://link.aps.org/supplemental/10.1103/PhysRevLett.132.120401, which includes further details on numerical calculations, an experimental proposal, additional examples, extended discussion of the role of dark states, and derivations of the critical exponents for the free fermion model, which includes Refs. [89–95].
[89] K. Mølmer and A. Sørensen, Phys. Rev. Lett. **82**, 1835 (1999).
[90] J. M. Torres, Phys. Rev. A **89**, 052133 (2014).
[91] T. Yoshida, K. Kudo, H. Katsura, and Y. Hatsugai, Phys. Rev. Res. **2**, 033428 (2020).
[92] B. Buča, C. Booker, M. Medenjak, and D. Jaksch, New J. Phys. **22**, 123040 (2020).
[93] M. Nakagawa, N. Kawakami, and M. Ueda, Phys. Rev. Lett. **126**, 110404 (2021).
[94] H. Yoshida and H. Katsura, Phys. Rev. A **107**, 033332 (2023).

[95] A. J. Daley, Manipulation and simulation of cold atoms in optical lattices, Ph.D. thesis, Leopold-Franzens-Universität Innsbruck, 2005.
[96] M. Zwolak and G. Vidal, Phys. Rev. Lett. **93**, 207205 (2004).
[97] F. Verstraete, J. J. García-Ripoll, and J. I. Cirac, Phys. Rev. Lett. **93**, 207204 (2004).
[98] T. Prosen and M. Žnidarič, J. Stat. Mech. (2009) P02035.
[99] G. De las Cuevas, N. Schuch, D. Pérez-García, and J. I. Cirac, New J. Phys. **15**, 123021 (2013).
[100] A. J. Daley, Adv. Phys. **63**, 77 (2014).
[101] J. Cui, J. I. Cirac, and M. C. Bañuls, Phys. Rev. Lett. **114**, 220601 (2015).
[102] E. Mascarenhas, H. Flayac, and V. Savona, Phys. Rev. A **92**, 022116 (2015).
[103] G. De las Cuevas, T. S. Cubitt, J. I. Cirac, M. M. Wolf, and D. Pérez-García, J. Math. Phys. (N.Y.) **57**, 071902 (2016).
[104] A. A. Gangat, I. Te, and Y.-J. Kao, Phys. Rev. Lett. **119**, 010501 (2017).
[105] A. Kshetrimayum, H. Weimer, and R. Orús, Nat. Commun. **8**, 1291 (2017).
[106] E. Gillman, F. Carollo, and I. Lesanovsky, New J. Phys. **21**, 093064 (2019).
[107] H. Weimer, A. Kshetrimayum, and R. Orús, Rev. Mod. Phys. **93**, 015008 (2021).
[108] A. A. Clerk, SciPost Phys. Lect. Notes 44 (2022).
[109] T. Manovitz, Y. Shapira, N. Akerman, A. Stern, and R. Ozeri, PRX Quantum **1**, 020303 (2020).
[110] T. Manovitz, Y. Shapira, L. Gazit, N. Akerman, and R. Ozeri, PRX Quantum **3**, 010347 (2022).
[111] Y. Shapira, T. Manovitz, N. Akerman, A. Stern, and R. Ozeri, Phys. Rev. X **13**, 021021 (2023).
[112] G. Albertini, S. R. Dahmen, and B. Wehefritz, J. Phys. A **29**, L369 (1996).
[113] For ease of visibility, the insets have $\kappa = 1.01J$ [65] (rather than $J/\kappa = 1$ as in the main plots), since the spectrum for open boundary condition reduces to a single point $\lambda = -J$ when $J = \kappa$.
[114] We note that a generic initial condition relaxes to an all down state $|{\Downarrow}\rangle$ rather than the spin-wave dark state $|D_{k_*}\rangle$, which can be understood as follows. Since there can be no transitions between the single magnon eigenstates, the only way to reach the dark state $|D_{k_*}\rangle$ is via quantum jumps from the two magnon sector. There are L linearly independent two magnon states that satisfy this requirement (see SM [88]). The remaining $\mathcal{O}(L^2)$ basis states will decay to the dark state with all spins down $|{\Downarrow}\rangle$, which is therefore the steady state for generic initial states at large L. Nevertheless, the dark state $|D_{k_*}\rangle$ plays a dynamical role that determines the asymptotic relaxation toward the all down state $|{\Downarrow}\rangle$.
[115] To reduce the impact of finite size effects, additional jump operators $\hat{L}_{1/L} = \sqrt{\kappa}\hat{S}^-_{1/L}$ are applied on the boundary sites, which ensures that the model has the same magnitude of on-site spin sinks (and sources) on all sites.
[116] N. Hatano and D. R. Nelson, Phys. Rev. Lett. **77**, 570 (1996).
[117] N. Hatano and D. R. Nelson, Phys. Rev. B **56**, 8651 (1997).
[118] P. Coleman, *Introduction to Many-Body Physics* (Cambridge University Press, Cambridge, England, 2015).
[119] The value for α and its uncertainty are obtained from a fit to data for the nonreciprocal XX model in Fig. 2(a). The exponents ν and z are determined by finding the best scaling collapse as assessed by the cost function λ defined in Ref. [120], with cubic spline data interpolation to generate the curves f_{n_j} and f_{C_j} respectively. Specifically, ν is determined from the collapse via Eq. (10) for the nonreciprocal XX model with 250 sites (data displayed in the SM [88]). The combination νz is determined from the collapse via Eq. (9), albeit for the XXZ model with 500 sites starting from $|{\Downarrow}\rangle$ [Fig. 3(a)]. Since z determines relaxation, we only consider data in the range $10^{-2.5} < (\Gamma/\kappa)(\kappa t)^{1/\nu z} < 10^0$, with the lower limit chosen to avoid transient timescales. Data for which $\Gamma > 0.01$ is ignored in this analysis, due to the larger distance from the critical point. This fixes z, with accompanying error propagation. The stated uncertainties are those for which the exponents $p \in \{\nu, z\}$ give a cost function $\lambda(p) = 2\lambda_{\min}$, where $\lambda_{\min}$ is the minimum of the cost function. If $\lambda_{\min} \approx 1$ in units of standard error, this aligns with the $\lambda(p) = \lambda_{\min} + 1$ uncertainty criterion of Ref. [121]. However, our criterion is not dependent on the exact value of the numerical error estimate, which from numerical testing we take to be $\delta C_j \sim 2.5 \times 10^{-6}$ and $\delta n_{j=475} \sim 10^{-4}$ for the respective cases discussed above. A basic procedure of minimization by least absolute difference (in log space) to the curve for the smallest Γ value gives $\nu = 0.385$ and $z = 1.97$.
[120] E. J. Dresselhaus, B. Sbierski, and I. A. Gruzberg, Phys. Rev. Lett. **129**, 026801 (2022).
[121] J. Houdayer and A. K. Hartmann, Phys. Rev. B **70**, 014418 (2004).
[122] N. Okuma and M. Sato, Phys. Rev. Lett. **126**, 176601 (2021).
[123] P. C. Hohenberg and B. I. Halperin, Rev. Mod. Phys. **49**, 435 (1977).